Characteristics of TMR Angle Sensors

Hiroshi Yamazaki, Hiraku Hirabayashi, Nobuya Oyama and Masanori Sakai
TDK CORPORATION
543 Otai, Saku-shi, Nagano, 385-8555 Japan

Background

Magnetic rotational angle sensors are widely used for detecting the angle of a motor, because of the advantages of non contact operation and no influence by oil sludge. As magnetic sensors, Hall effect sensors and anisotropy magnetoresistive (AMR) sensors are commercialized and used in various applications.

Tunneling magnetoresistive (TMR) angle sensors were developed and evaluated. Here is a report of the TMR angle sensors.

Feature and principle

There are many advantages in using TMR for angle sensors. First, the MR ratio of TMR is very high. [1], [2], [3], [4], [5] Consequently, the signal output can be greatly higher than other magnetic sensors. Because of the current-perpendicular-to-plane structure (CPP), wide variation of the shape of the magnetic tunnel junction (MTJ) can be adopted compared to GMR (giant magnetoresistive) and AMR with the current-in-plain structure (CIP). In addition, it is also one of the favorable features that the frequency response to the magnetic flux change is fast, which is demonstrated by being used as hard disk drive (HDD) heads. It is well known that HDD which operates at high data transfer rates is using TMR technology.

Fig. 1 shows the schematic diagram of the operation of the TMR angle sensor. TMR has the spin valve (SV) structure consists of the pinned layer, the barrier layer and the free layer. The magnetization of the free layer rotates to align

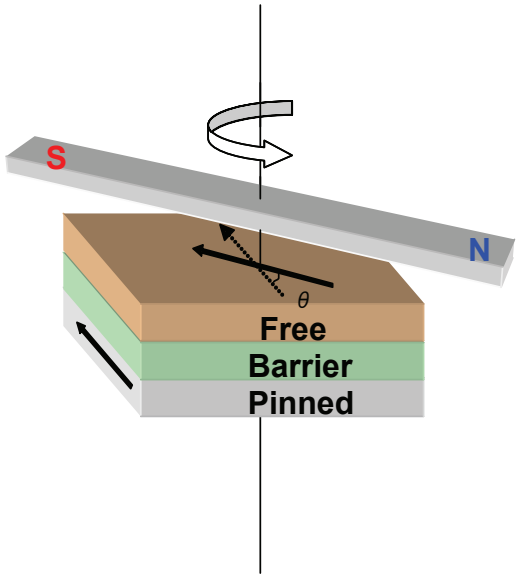

Fig. 1 TMR sensor operation conceptual diagram

with the direction of the applied magnetic field. The change of the angle between the pinned layer magnetization and the free layer magnetization causes the change of the TMR resistance.

Fig. 2 shows the bridge set-up of the angle sensor. It consists of two Wheatstone bridges where the direction of the pinned layer is mutually orthogonal as shown in the figure. One bridge outputs the COS signal, and the other outputs the SIN signal. The arrow in the figure indicates the direction of the magnetization of the pinned layer. For R1 and R2 and also for R3 and R4, the direction of the pinned layer magnetization is mutually anti-parallel. Vcos is obtained from one bridge (COS bridge), Vsin is obtained from the other bridge (SIN bridge), and θsens is given by the arc tangent of the ratio of them as shown in the equations (1)-(3).

$$\theta_{sens} = \arctan\left(\frac{V_{\sin}}{V_{\cos}}\right) \quad (1)$$

$$V_{\cos} = V_{cc} \times \left(\frac{R_3(\theta)}{R_3(\theta)+R_4(\theta)} - \frac{R_2(\theta)}{R_1(\theta)+R_2(\theta)}\right) \quad (2)$$

$$V_{\sin} = V_{cc} \times \left(\frac{R_7(\theta)}{R_7(\theta)+R_8(\theta)} - \frac{R_6(\theta)}{R_5(\theta)+R_6(\theta)}\right) \quad (3)$$

Here, Vcc is applied voltage to the bridges. $R_i(\theta)$ (i = 1-4) is the resistance of the COS bridge, and $R_i(\theta)$ (i = 5-8) the resistance of the SIN bridge. They are also the function of the temperature. θ_{sens} is the detected angle.

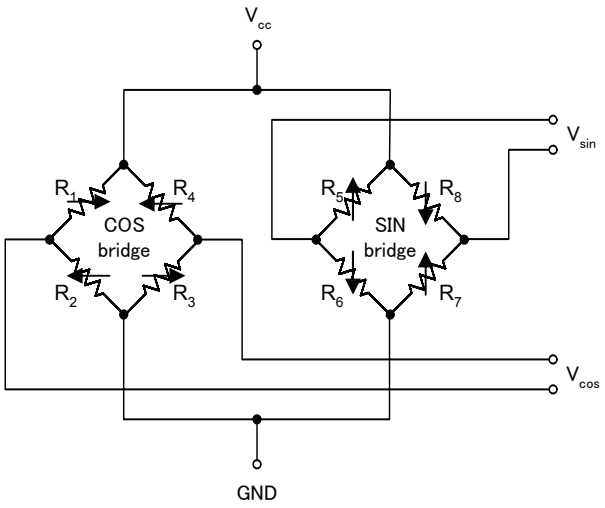

Fig. 2 Angle sensor bridge structure

Composition

TMR is formed by the DC magnetron sputtering method in the order of deposition of the under electrode, the pinned layer, the barrier layer, the free layer and the upper electrode. An anti-ferromagnetic layer was adopted to pin the magnetization direction of the pinned layer.

The shape with small shape-anisotropy was adopted so that the magnetization direction of the free layer can follow a weak magnetic field without being hindered. The bridge circuit was formed by using normal photolithography.

The applied voltage was 5V. The amplitude was measured at room temperature, and the angle error was calculated.

Sensor characteristic

Fig. 3 shows an example of the output signal waveform. At room temperature, the output reaches 3000mV.

Fig. 4 shows an example of the dependence of the difference of the angle error on the rotation direction. The influence of hysteresis is very small, and the angle error is about 0.1 degrees.

Next, the dependence of the angle error on the magnetic field strength is shown in Fig. 5. The minimum value of the angle error exists at about 60mT of the magnetic field, and it is smaller than 0.3 degrees over the range of 10mT-70mT, which indicates that this sensor will be used in various

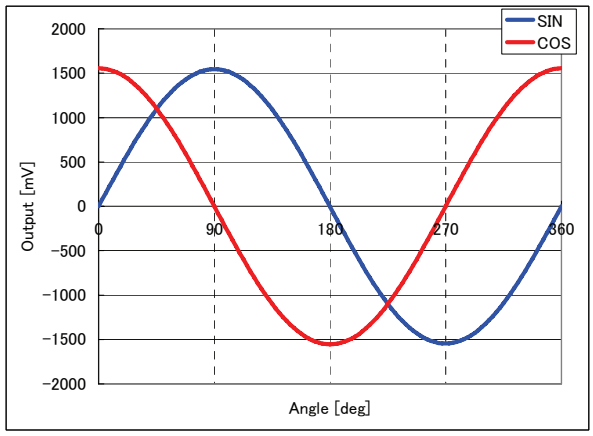

Fig. 3 Power waveform of TMR sensor

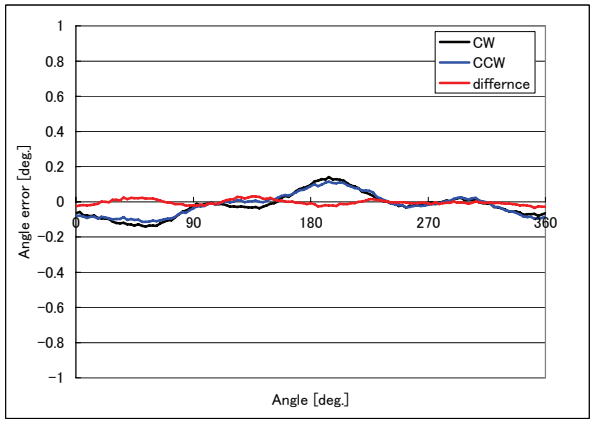

Fig. 4 Difference of angle error by the rotation direction

magnetic field strength conditions. These favorable characteristics were achieved by the decrease of coercive force and magnetic anisotropy of the free layer, the optimization of the pinned layer and the shape with the small shape-anisotropy.

Fig. 6 shows the frequency response of the angle error of the same chip structure. No change is observed over the range of from 100rpm to 3000rpm, which is noteworthy.

Next, the temperature dependence was examined over the practical range of from -40degC to 125degC. We measured the temperature dependence of the offset, the angle error and the output as shown in Fig. 7. The temperature dependence of the offset is confined within a small range of +/-1mV. The offset ratio which is the offset divided by TMR output voltage becomes about 0.033%. If the offset change is assumed to be +/- 1mV here, the offset ratio of GMR and AMR becomes 0.21% and 0.68%, respectively. Fig. 8 shows the comparison between TMR, GMR and AMR of the angle error variation over the temperature range of from -40 degC to 150 degC when the sensor output is adjusted to the same value.

The angle error increases about 0.2 degrees in high and low temperature. The output tends to decrease along with the temperature rise. The

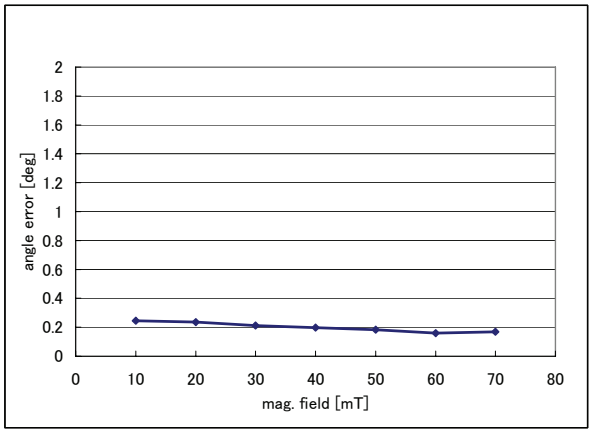

Fig. 5 Magnetic field strength dependence of the angle error

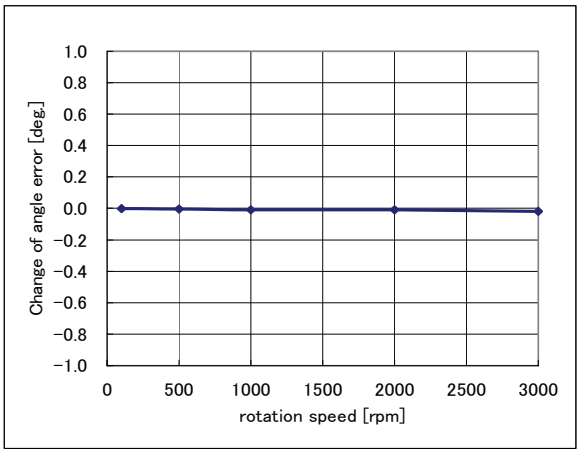

Fig. 6 Frequency dependence of the angle error

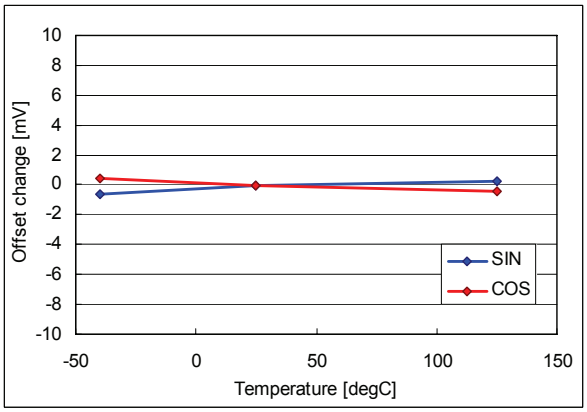

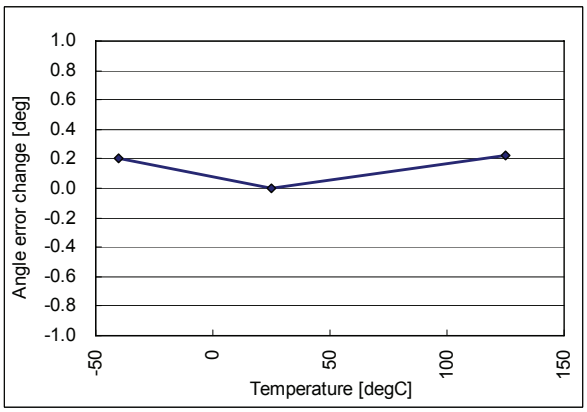

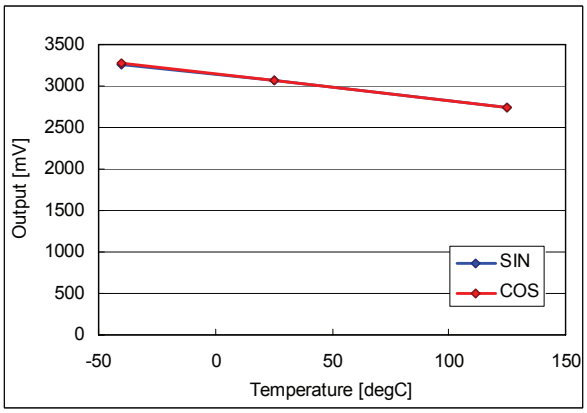

Fig. 7 Temperature dependence of offset, angle error and output

temperature coefficient is about -3.18mV/degC, and -0.11%/degC when shown by the percentage of the output at room temperature.

Barrier reliability

The lifetime of the TMR barrier layer was estimated by the same method as being used for HDD heads.

Generally, the electrical breakdown of the TMR barrier layer is mainly caused by pinhole enlargement where the pinholes in the barrier oxide film gradually enlarge (Soft Breakdown). For the HDD heads, the lifetime of the barrier layer is calculated by the IPL(Inverse Power Law) model. Delta MR resistance (dMRR) is the change of the TMR barrier resistance over time, and the relationship between the time at which dMRR reaches -1% (T_d) and the applied voltage (V_{TMR}) is shown in Fig. 9. It is shown that it takes 6×10^{10} years for resistance to decrease by 1% under 5V supply and 150degC conditions. The TMR barrier layer shows long lifetime and enough reliability.

Environmental robustness

Finally the environmental aspects are evaluated. An electrostatic discharge (ESD) examination was conducted for the sensor which includes the protective structure inside its element. Fig. 10 shows the test result in human body model (HBM). No resistance change was observed up to 8kV, and it was confirmed the effectiveness of the protective structure.

The test result of the external magnetic field robustness is shown in Fig. 11. The external magnetic field up to 1000mT was applied to the sensor, and the characteristics after removal of the magnetic field were measured. No change of the angle error by the external magnetic field was observed and the high external magnetic field robustness was demonstrated.

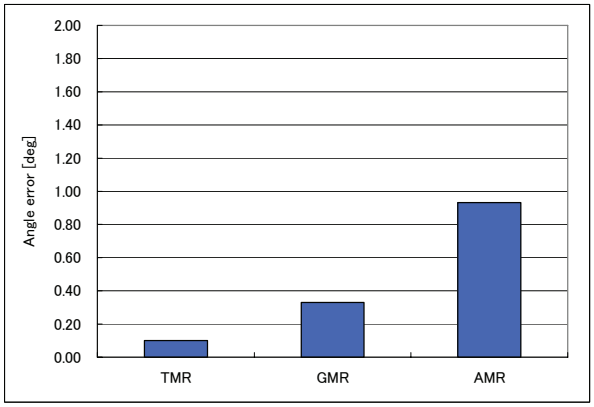

Fig. 8 Comparison of the angle error variations

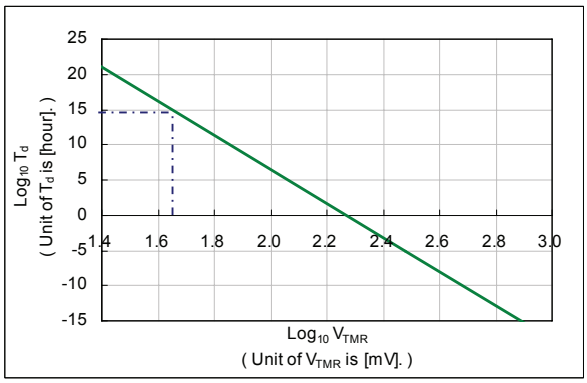

Fig. 9 Barrier life prediction

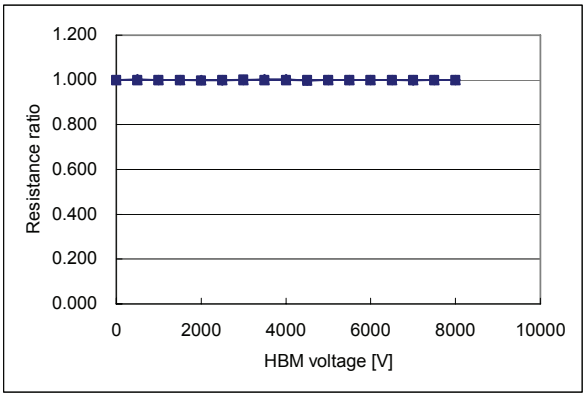

Fig. 10 ESD testing

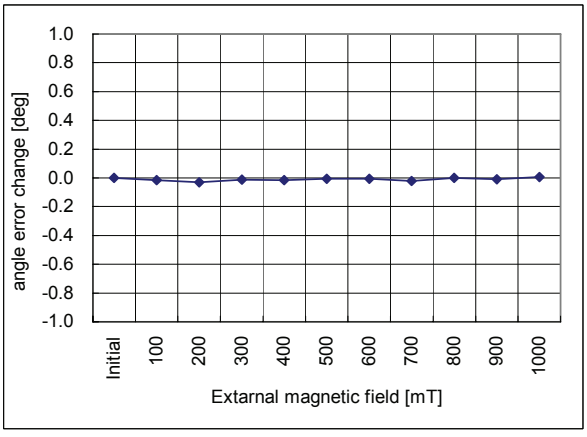

Fig. 11 External magnetic field robustness

Summary

We have evaluated the TMR angle sensor.

For the structure that consisted of two orthogonal Wheatstone bridges, the angle error was smaller than 0.3 degrees over the magnetic field range of 10mT-70mT. In addition, the offset change was within the range of +/-1mV (Vcc=5V) and the angle error increase was 0.2 degrees at the maximum over the temperature range of from -40degC to 125degC.

It was confirmed longer than 100 years of the life prediction, 8kV or higher ESD (HBM) insusceptibility and the higher than 1000mT external magnetic field robustness.

Acknowledgement

We wish to express our gratitude to the members of the group for their collaboration in development, device fabrication, evaluation, film development, device design, process design and reliability evaluation as this report was being prepared.

Reference

[1] M. Julliere, “Tunneling between Ferromagnetic Films”, Phys. Lett. A 54, 225 (1975).

[2] J.S. Moodera, et al., “Large Magnetoresistance at Room Temperature in Ferromagnetic Thin Film Tunnel Junctions”, Phys. Rev. Lett. 74, 3273 (1995).

[3] T. Miyazaki and N. Tezuka, ”Giant Magnetic Tunneling Effect in Fe/Al2O3/Fe Junction”, J. Magn. Magn. Mat. 139, L231 (1995).

[4] T. Kuwashima, et al., “Electrical Performance and Reliability of TuMR Heads for 100Gb/in2 Application”, IEEE Trans. Magn., 40, 176 (2004).

[5] T. Kagami, et al., “A Performance Study of Next Generation’s TMR Heads Beyond 200 Gb/in2”, IEEE Trans. Magn., 42, 93 (2006).